ACADEMIC PRESS

Archives of Biochemistry and Biophysics 406 (2002) 153–164

ABB

www.academicpress.com

Effects of TCDD upon IκB and IKK subunits localized in microsomes by proteomics

Maribel E. Bruno,[a] Christoph H. Borchers,[b] J. Michael Dial,[b] Nigel J. Walker,[c] Jennifer E. Hartis,[a] Barbara A. Wetmore,[a] J. Carl Barrett,[d] Kenneth B. Tomer,[b] and B. Alex Merrick[a,*]

[a] *Proteomics Group, National Center for Toxicogenomics, National Institute of Environmental Health Sciences, P.O. Box 12233, Research Triangle Park, NC 27709, USA*

[b] *Mass Spectrometry Group, Laboratory of Structural Biology, National Institute of Environmental Health Sciences, P.O. Box 12233, Research Triangle Park, NC 27709, USA*

[c] *Environmental Toxicology Program, Laboratory of Computational Biology and Risk Analysis, National Institute of Environmental Health Sciences, P.O. Box 12233, Research Triangle Park, NC 27709, USA*

[d] *Laboratory of Molecular Carcinogenesis, National Institute of Environmental Health Sciences, P.O. Box 12233, Research Triangle Park, NC 27709, USA*

Received 10 June 2002, and in revised form 17 July 2002

Abstract

Biochemical studies have shown that microsomes represent an important subcellular fraction for determining 2,3,7,8-tetrachlorodibenzo-*p*-dioxin (TCDD) effects. Proteomic analysis by two-dimensional gel-mass spectrometry of liver microsomes was undertaken to gain new insight into the actions of TCDD in male and female rats. Proteomic analysis showed TCDD induced several xenobiotic metabolism enzymes as well as a protein at 90 kDa identified by mass spectrometry as IκB kinase β/IKK2. This observation led to the discovery of other NF-κB binding proteins and kinases in microsomes and effects by TCDD. Western blotting for IKK and IκB family members in microsomes showed a distinct pattern from cytosol. IKK1 and IKK2 were both present in microsomes and were catalytically active although, unlike cytosol, IKKγ/NEMO was not detectable. TCDD exposure produced an elevation in cytosolic and microsomal IKK activity of both genders. The NF-κB binding proteins IκBβ and IκBγ were prevalent in microsomes, while IκBα and IκBε proteins were absent. TCDD treatment produced hyperphosphorylation of microsomal IκBβ in both sexes with females being most sensitive. In cytosol, IκBα, IκBβ, and IκBε, but not IκBγ, were clearly observed but were not changed by TCDD. Overall, proteomic analysis indicated the presence of NF-κB pathway members in microsomes, selectively altered by dioxin, which may influence immune and inflammatory responses within the liver. Published by Elsevier Science (USA).

Keywords: IκB; IKK; Liver; Microsomes; NF-κB; Proteomics; Rat; TCDD

One of the most potent inductions of metabolic enzymes in liver is mediated by the ligand–receptor interaction of 2,3,7,8-tetrachlorodibenzo-*p*-dioxin (TCDD)[1] and the arylhydrocarbon receptor (AhR). Increased mRNA and protein expression of microsomal cytochrome P-450 (CYP)1A1, 1A2, 1B1, and several phase

* Corresponding author. Fax: 1-919-541-4704.

E-mail address: merrick@niehs.nih.gov (B. Alex Merrick).

[1] *Abbreviations used:* ER, endoplasmic reticulum; AhR, arylhydrocarbon receptor; TCDD, 2,3,7,8-tetrachlorodibenzo-*p*-dioxin; CYP, cytochrome P-450; NF-κB, nuclear factor-κB; IκB, Inhibitor κB; IKK, IκB kinase; NEMO, NF-κB Essential Modulator; Ig, immunoglobulin; TNFα, tumor necrosis factor α; DTT, dithiothreitol; 2D, two dimensional; IEF, isoelectric focusing; IPG, immobilized pH gradient; SDS, sodium dodecyl sulfate; CBB, Coomassie brilliant blue; Rb, retinoblastoma; Grp, glucose regulated protein; H-ras, Harvey-ras; GST, glutathione S-transferase; HRP, horseradish peroxidase; ECL, enhanced chemiluminescence; SDS–PAGE, sodium dodecyl sulfate–polyacrylamide gel electrophoresis; MS, mass spectrometry; MALDI/TOF, matrix-assisted laser desorption–ionization/time of flight; ESI, electrospray ionization; p*I*, isoelectric point; Hsp, heat shock protein; SOD, superoxide dismutase; IL1α, interleukin 1α; TRX/ADF, thioredoxin/adult T-cell leukemia-derived factor.

0003-9861/02/$ - see front matter. Published by Elsevier Science (USA).
PII: S0003-9861(02)00452-6

II conjugation enzymes provide sensitive and tissue-specific indicators of exposure to TCDD and related polyhalogenated aromatic compounds [1]. Prolonged induction of cytochrome P450 monooxygenases during chronic TCDD exposure is a likely critical component in its carcinogenic action even though TCDD is not directly genotoxic. Increased CYP1 isozyme-mediated metabolism is hypothesized to form excessive reactive oxygen species leading to DNA damage and cancer [2–4]. Another facet of TCDD toxicity is the sex-related selectivity that is evident in some animal models; for example, TCDD can be a potent hepatocarcinogen in female rats but not in males [5,6]. Recent evidence has shown an estrogen-dependent induction of 8-oxo-deoxyguanosine adducts in female rats by TCDD, supporting the notion of a prolonged oxidative imbalance that occurs in a sex-dependent manner [4]. Other studies have shown that overexpression of antioxidants such as the thioredoxin, TRX/ADF, provide protection against TCDD-induced hematotoxicity, indicating that reactive oxygen species may play a role in nonhepatic dioxin toxicity [7]. Ultrastructural studies of female rat liver after TCDD exposure have also revealed an increase in smooth endoplasmic reticulum (ER) [8]. These data indicate that the microsomal fraction is important for studying TCDD action where sex-specific effects and the cellular redox state may play an important role.

Cells respond to changing internal and environmental stimuli by adjustments in gene expression mediated by many inducible transactivating factors including nuclear factor-κB (NF-κB). The association between oxidative stress and NF-κB activation remains an area of intense study [9]. NF-κB transactivates a variety of genes regulating immune, inflammatory, developmental, and cell survival responses [10–13]. The predominant form of NF-κB in most cells is a heterodimer composed of the subunits, p65/RelA and p50/NF-κB1. In the resting state, NF-κB is inactive and bound in the cytoplasm by an inhibitor binding protein (IκB) that can exist as several isoforms including IκBα, β, γ, ε, and δ or in the nucleus as IκBζ [14,15]. NF-κB activation involves rapid phosphorylation of IκB proteins at two conserved serines in the amino terminus, and subsequent release of NF-κB for transport to the nucleus and transcription of target genes [16,17]. The most abundant inhibitory protein, IκBα, undergoes ubiquitination and proteasomal degradation when phosphorylated at Ser^{32} and Ser^{36}. The kinase responsible for IκB phosphorylation is the IκB kinase (IKK) signalsome consisting of two catalytic subunits, IKK1/α and IKK2/β, and a structural subunit IKKγ/NEMO (NF-κB Essential Modulator) [14]. Regulation of the signal-dependent functions of IKK remains an active area of investigation.

Recent studies have explored a possible connection between the AhR pathway and NF-κB activation because of their mutual involvement in regulation of oxidative stress, immunoresponsiveness, cell survival, and cell proliferation [18–20]. Studies examining the immunosuppressive nature of TCDD demonstrated inhibition of IgM expression in B-cell lymphoma cells that was mediated by AhR activation and by dioxin response elements found in the immunoglobulin (Ig) heavy chain promoter region [18]. However, the concurrent induction of NF-κB/Rel proteins by TCDD was neither AhR-dependent nor sustained in vivo [18]. In Hepa1c1c7 mouse hepatoma cells, the activated AhR binds to the NF-κB subunit, p65, but not the p50 subunit, and blocks tumor necrosis factor α (TNFα)-initiated activation of p50–p65 dimers and transcriptional activation of an NF-κB reporter gene [19]. Experiments in the same cell line demonstrated that TCDD produced a sustained activation of NF-κB made up of p50 homodimers, not p50–p65 complexes, in which the former have been associated with repression of gene transcription [21]. These in vitro modulations in the NF-κB pathway are thought to result from an oxidative signal brought about by AhR activation and increased CYP1A1 activity [21]. However, TCDD toxicity has not been linked to the NF-κB pathway in in vivo studies.

Proteomics represents a series of technologies for global analysis of protein expression from a cellular genome or from a particular subcellular organelle [22]. While the cellular genome is relatively stable, a proteome constantly adapts to changes in the cellular environment. A key proteomic technology for studying protein expression response is the coupling of 2D gel separation with protein identification by mass spectrometry [23]. This method has often been used to examine differential protein expression in whole cell lysates or organ homogenates. The isolation of microsomes by ultracentrifugation provides an effective means to enrich for ER, which can then be examined for protein expression changes that might occur after TCDD exposure. Further, ultrastructural studies of liver from rats exposed to TCDD reported an increase in smooth ER profiles and a corresponding decrease in rough ER [8]. During proteomic analysis of microsomal fractions, we observed the presence of IKK2. Since this finding had not been previously reported, it led us to determine expression of other members of the IKK and IκB families in microsomal proteins isolated from male and female rats. Subsequent analysis showed a distinct expression pattern of IKK and IκB family members in microsomes compared to cytosol that was affected by TCDD treatment and sex. Further, IKK1,2 found in microsomes was found to be catalytically active which was enhanced by TCDD. These results demonstrate the potential influence of a membrane-bound NF-κB pathway that may contribute to the cellular response of TCDD and perhaps other chemical exposures.

Materials and methods

Animals and housing

Twelve-week-old male and female Sprague–Dawley rats were obtained from Charles River (Raleigh, NC) and were acclimated on a 12-h light–dark cycle for at least 1 week prior to treatment. Animals were housed under controlled temperature (70 ± 0.5 °F) and humidity ($50 \pm 5\%$) conditions at three per cage and allowed free access to food and water. Rats were treated with a single dose of vehicle or 25 μg/kg of TCDD (Dow Chemical, Midland, MI) by oral gavage in corn oil at 2 ml/kg ($n = 3$ rats/group). After 72 h, animals were euthanized by carbon dioxide inhalation and liver samples were removed within 2 min of death, minced, placed in cryovials, and quick-frozen in liquid nitrogen. Quick-freezing did not affect the subcellular distribution of proteins concerned in this study (unpublished observations). After freezing, samples were stored at −70 °C.

Isolation of microsomes

Rat livers were thawed and homogenized in a glass mortar and Teflon pestle with 5 volumes of lysis buffer (50 mM Hepes pH 7.5, 1 mM EDTA, 0.25 M sucrose, 1 mM DTT, and protease inhibitor cocktail (Calbiochem, La Jolla, CA). Liver homogenates for each animal were centrifuged at 10,000*g* for 20 min at 4 °C to remove nuclei, mitochondria, and debris and the supernatants recentrifuged to remove residual mitochondria. The 10,000*g* supernatants were centrifuged at 100,000*g* in a Beckman Ultracentrifuge (Palo Alto, CA) for 1 h at 4 °C to pellet microsomes. The microsomal fraction was washed by gentle rehomogenization and resuspension prior to a second ultracentrifugation. Consistent with the findings of others [24], we found that direct solubilization of freshly isolated microsomal lipoproteins allowed complete protein solubilization in a urea-based 2D gel buffer. Preliminary studies in our lab showed that dialysis and lyophilization of microsomal lipoproteins to remove ions and concentrate protein prior to isoelectric focusing (IEF) produced incomplete protein solubilization and poor electrophoretic separation. It was also important to completely solubilize microsomal lipoproteins in a nonionic native lysis buffer that was compatible with kinase assay conditions.

Protein separation by two-dimensional (2D) gels and image analysis

Microsomal proteins were directly solubilized in urea-based buffer (7 M urea, 2 M thiourea, 4% 3-[3-cholamidopropyl)dimethylammonio]-1-propane-sulfonate (CHAPS), 40 mM Tris, 1% Tergitol-10, 0.5% *n*-octyl-β-glucopyranoside, 50 mM dithiothreitol, 2 mM tributylphosphine, 0.5% ampholytes pH 3–10, trace bromophenol blue) prior to IEF. Protein concentration was determined by the bicinchinoic acid method (Pierce, Rockford, IL) from 5% trichloracetic-acid-washed protein precipitates that were solubilized in 1 M sodium hydroxide. IEF was performed in an equilibrium mode using an immobilized pH gradient (IPG) on an IPGphor apparatus (Amersham Biosciences, Piscataway, NJ) on 18 cm IPG strips, pH 3–10 (Amersham Biosciences). IPG strips were hydrated for 12 h at 50 V/h and then focused at 500 V for 1 h, 1000 V for 1 h, and 8,000 V for 4 h for a total of about $35,000\ \mathrm{V} \cdot \mathrm{h}$. After IEF, the IPG strips were reduced and alkylated in two successive 15-min washes in an equilibration buffer (50 mM Tris–HCl, pH 8.8, 6 M urea, 30% glycerol, 2% SDS, trace of bromophenol blue) containing first 10 mg/ml DTT, then 25 mg/ml iodoacetamide. Separation of proteins by mass was performed in 1-mm-thick acrylamide gels cast in an 8–16% gradient and separated at 50 mA in a running buffer composed of 50 mM Tris, pH 8.3, 196 mM glycine, and 0.1% SDS. Gels were fixed for 0.5 h in an aqueous solution of 10% acetic acid and 25% isopropanol with staining overnight in an aqueous solution of 0.01% colloidal Coomassie brilliant blue (CBB) G stain (BioRad, Richmond, CA), 10% acetic acid, and 10% ethanol solution. Destaining took place with three washes of an aqueous solution of 10% acetic acid and 10% isopropanol.

Stained gels were scanned (Agfa, Ridgefield, NJ; Arcus scanner) as TIFF images at 300 dpi and were analyzed using PDQuest software (BioRad, Richmond, CA). Six images per sex ($n = 3$/control and TCDD) were analyzed. After subtraction of background noise and streaking, gels were then assigned to a matchset and a representative control gel was selected as the standard gel. Fold change for each protein was determined in control versus TCDD treatments for males and females.

Antibodies and western blotting

A rabbit polyclonal antibody that detects both rat CYP1A1/CYP1A2 isoforms was produced as previously described [25]. A rabbit polyclonal antibody for 25-DX protein was raised against the peptide (-LKDEYDDLSDLTPA-), which corresponds to amino acids 135–148 predicted for the rat 25-DX sequence [26] and was kindly provided by Dr. Douglas Bell (NIEHS, NC). IKK1, IKK2, IKKγ/NEMO, IκBα, IκBβ, IκBε, IκBγ, retinoblastoma (Rb) protein, and Bcl2 were rabbit host polyclonal antibodies, a goat polyclonal antibody was used for glucose-regulated protein, (Grp)78, and a mouse monoclonal antibody was directed against p65/NF-κB that were purchased from Santa Cruz Biotechnology (Santa Cruz, CA).

Mouse monoclonal antibodies were obtained for Harvey-ras protein (H-ras) (Santa Cruz Biotech) and GM130 protein (BD Signal Transduction Labs, San Diego, CA). Rat kidney KNRK cell lysate and rat cerebrum lysate were used as positive controls for H-ras and GM130 proteins, respectively. Goat anti-GST Ya polyclonal antibody was obtained from Oxford Biomedical Research (Oxford, MI). Rabbit and mouse IgG were purchased from Calbiochem (San Diego, CA). Horseradish peroxidase (HRP)-conjugated secondary antibodies were obtained for mouse and rabbit IgG from Amersham Biosciences (Piscataway, NJ) and goat IgG was from Roche Biochemicals (Indianapolis, IN). Enhanced chemiluminescence (ECL) reagents were purchased from Amersham Biosciences.

For western blotting, microsomal protein samples from each rat were solubilized, separated by sodium dodecyl sulfate–polyacrylamide gel electrophoresis (SDS–PAGE), and blotted onto nitrocellulose for immunodetection as previously described [27]. Briefly, 25–50 μg of microsomal proteins were separated on 8–16% gradient minigels and then transferred onto nitrocellulose by the tank method using Towbin's solution. Immunodetection of HRP-labeled secondary antibodies was performed with ECL reagents. For some blots, densitometry (Molecular Dynamics personal densitometer, Foster City, CA) of scanned ECL films was performed for quantitative comparison of results.

Mass spectrometry

Samples for gel excision were selected for mass spectrometry (MS) analysis based either on a 1.5-fold difference from the control determined by image anal-

Table 1
Identification of rat liver microsomal proteins following 2D gel separation and MALDI/TOF MS analysis

Spot no.	Protein identification[a]	M_r[b]	p*I*[b]	NCBI accession no.	% aa coverage[c]	Est'd. *z*[c]	No. matched peptides[c,e]
1	150 kDa oxygen-regulated protein	150.0	5.1	1480453	8	1.53	7/8
2	IKB kinase-β (IKK2)	86.9	5.9	6650707	6	0.33	4/8
3	78 kDa glucose-regulated protein precursor	72.3	5.1	121574	15	2.43	7/9
4	DNA K-type molecular chaperone hsp72-psl	70.9	5.4	347019	14	2.43	6/9
5	Rat serum albumin precursor	68.7	6.1	113580	13	2.11	6/6
6	Calreticulin precursor (CRP55)	48.0	4.3	117505	7	2.00	4/8
7	Iodothyronine 5′ monodeiodinase	54.1	4.9	202549	19	2.41	8/8
8	Protein disulfide isomerase ER60 precursor	56.6	5.9	1352384	18	2.39	7/12
9	Glutamate dehydrogenase	61.4	8.3	56198	8	2.04	4/6
10	ATP synthase beta subunit	51.2	4.9	1374715	20	2.43	6/6
11	Isocitrate dehydrogenase (NADP)	46.7	6.5	1170478	13	2.26	5/8
12	Cytochrome P450 2D4	56.7	6.9	117244	8	2.25	3/17
13	3-α-Hydroxysteroid dehydrogenase (3-α-HSD)	37.05	7.1	236058	22	2.42	6/8
14	Glyceraldehyde-3-phosphate dehydrogenase	35.8	8.4	8393418	10	1.65	3/5
15	25-DX	24.65	4.4	11120720	23	2.43	5/5
16	Prohibitin	29.8	5.6	130020	12	1.66	3/4
17	PRxIV	31.0	6.2	4336879	14	1.72	3/3
18	Endoplasmic reticulum protein ERP29 precursor	28.6	6.2	2507015	15	1.50	5/7
19	Glutathione S-transferase Yb2	22.83	7.0	207692	29	1.67	4/6
20	Glutathione S-transferase alpha	25.97	9.0	7188365	13	2.43	4/6
21	Cytochrome B5	14.3	4.9	231928	32	2.43	4/8
22	Ferritin light chain	20.8	6.0	2119695	34	2.43	4/6
23	Cu/Zn SOD[d]	16.0	5.7	1213217	15.6	Verified by Q-TOF[d]	

[a] Protein names are listed as they appear in the NCBI database.
[b] M_r and p*I* were calculated from the predicted amino acid sequence for each protein.
[c] See Materials and methods for information.
[d] Initial MALDI/TOF analysis suggested that this protein was Cu/Zn SOD but overall data were inconclusive. Subsequent analysis by Q-TOF MS confirmed the identity of Cu/Zn SOD.
[e] The three major ions in mass spectrum of spot no. 12 were consistent with cytochrome P450 2D4 with a *z* score of 2.25, while the remaining minor ions were not identifiable.

ysis or on their prominence as landmark proteins in the gel. Stained proteins were excised manually with sterile glass pipets and automated in-gel trypsin digestion was performed according to the manufacturer's protocol using a ProGest workstation (Genomics Solutions, Ann Arbor, MI). Mass calibration was performed either externally by a calibration mix bracketing the ions of interest or internally using trypsin peptides of known mass. Mass accuracy was better than 30 ppm. The digests were lyophilized and mass spectral analysis was performed on a Voyager DE-STR matrix-assisted laser desorption–ionization time-of-flight (MALDI/TOF) spectrometer (PerSeptive Biosystems, Framingham, MA) with delayed ion extraction in the reflector mode with an accelerating voltage of 20 kV and a 3.0-m flight path. A 337 nm nitrogen laser was used to desorb and ionize samples. Samples were prepared for MALDI by the dried-droplet method with a saturated solution of recrystallized α-cyano-4-hydroxycinnamic acid in ethanol:water:formic acid. All electrospray ionization (ESI) MS–MS analyses were performed on a Q-TOF hybrid mass spectrometer (Micromass, Altrincham, UK) equipped with a nebulized nanospray electrospray source (nanoflow-ESI/MS). Critical ions were searched against the Prospector (http://prospector.ucsf.edu/UCSF, San Francisco, CA) and Profound databases (http://prowl.rockefeller.edu/cgi-bin/ProFound, Rockefeller University, New York, NY) for identification. The percent of amino acid coverage represents the portion of the protein containing matching tryptic fragments from MALDI-MS. The estimated z score (see Table 1) is an indicator of protein identification and corresponds to the percentile of the result in the random match population. A protein with a 'z' score of 1.645 indicates that the database search for the designated protein identity is in the 95th percentile, and 5% random matches remain that could yield higher z scores. A greater z score relates to higher confidence of protein identification.

IKK kinase assay

In vitro assay for IKK kinase was adapted from published procedures [27,28]. Briefly, IKK1,2 antibody (H-470 rabbit polyclonal, Santa Cruz, CA) was bound to IKK1 and IKK2 catalytic subunits from cytosol or solubilized microsomes. The immune complex was immunoprecipitated and washed. IKK kinase assay was performed using recombinant IκBα as a full length substrate (1–317, sc-4094; Santa Cruz, CA) with 200 μM ATP and 10 μCi ^{32}P-ATP for 20 min at 30 °C. ^{32}P-labeled product was separated on a 4–20% minigel, fixed, impregnated with Amplify (Amersham BioSci., Piscataway, NJ), dried, and exposed to film for 12 h at −80 °C. Rabbit IgG was used as a negative control during immunoprecipitation.

Results

Homogeneity of microsomes

The relative homogeneity of microsomes was determined by western blotting for organelle-specific proteins (Fig. 1). The presence of the ER resident protein, Grp78, served as a positive ER marker protein and was observed in all microsomal fractions. Maturation of proteins occurs after biosynthesis at the ER and transport to the Golgi apparatus for which GM130 is a resident structural element also detected in the microsomes [29]. Other representative proteins from mitochondria (Grp75, Bcl-2), nuclei (Rb), plasma membrane (H-ras), and cytosol (p65 NF-κB) were absent from the microsomal preparation. These data suggest that microsomes were enriched for ER and Golgi in each preparation by current isolation procedures with minimal levels of contamination by the other cellular organelles or cytosolic proteins that were surveyed.

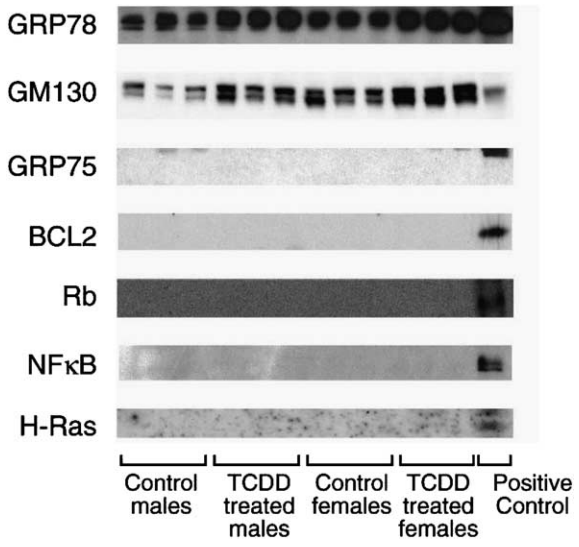

Fig. 1. Western blot analysis to determine homogeneity of microsomal fractions from rat liver. Male and female Sprague–Dawley rats were orally gavaged with vehicle and TCDD for 72 h prior to isolation of liver microsomes. Organelle-specific antibodies were used to confirm the absence of organelle proteins or presence of resident protein in the microsomal fraction from each animal at $n = 3$ per group. The microsomal-specific protein, GRP78, and Golgi-specific protein, GM130, were present in all microsomal samples. In addition, these two proteins were not detectable in cytosol (data not shown). Mitochondrial-specific proteins (GRP75 and Bcl-2), nuclear-specific protein (Rb), nuclear and cytosolic protein (p65/NFκB), and the plasma membrane protein (H-ras) were uniformly absent from each microsomal preparation. Positive control proteins were generally prepared from the rat subcellular fraction of interest for each blot. Each lane contained solubilized microsomal protein from an individual animal.

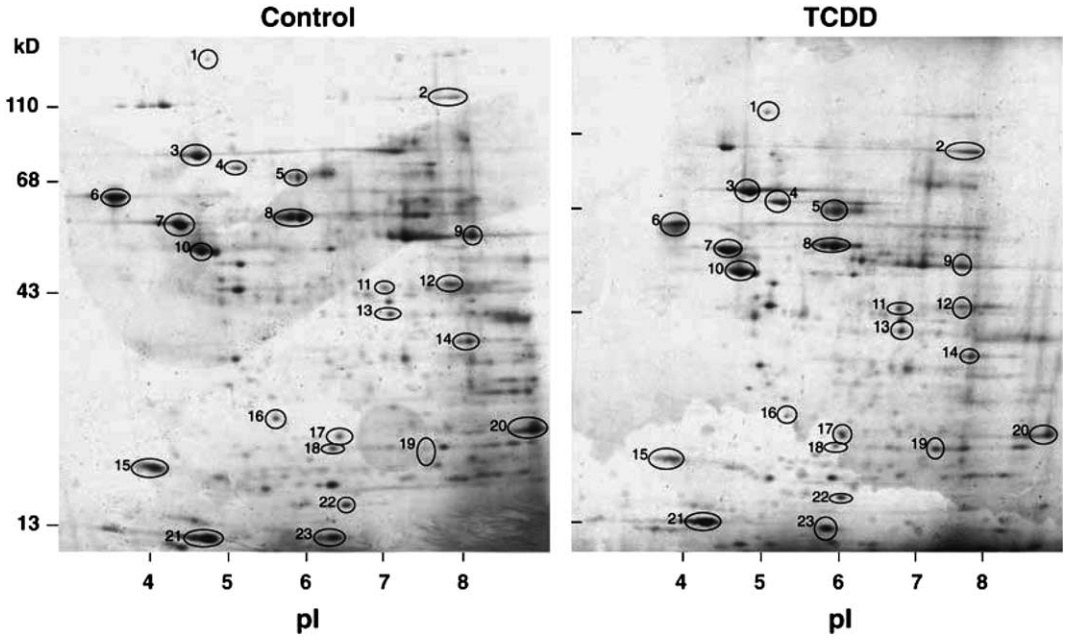

Fig. 2. 2D gel separation and detection of rat liver microsomal proteins after acute control and TCDD treatments. A 300-μg amount of liver microsomal proteins was separated by 2D gel analysis according to Materials and methods. Shown here is a representative control and TCDD gel from female rats. Each sample was run in duplicate. Separated proteins were detected using colloidal Coomassie brilliant blue stain. Proteins were excised, digested with trypsin, and analyzed by MALDI/TOF MS analysis for protein identification by mass fingerprinting. Numbered proteins in gels correspond to the identified proteins contained in Table 1 and fold changes in Fig. 3.

Proteomic analysis of microsomal proteins

Microsomal proteins were solubilized, separated by 2D gel electrophoresis, stained with colloidal CBB, and image analyzed for protein differences between control and TCDD-treated male and female rats. Microsomal samples were prepared for each animal to maintain the individual microsomal protein profile. One gel for each animal was image analyzed for a total of three microsomal images per group. Despite the membranous environment and lipid-rich nature of the microsomes, proteins separated reasonably well within the isoelectric range of pH 4–9 as seen in Fig. 2. Some horizontal streaking occurred with proteins possessing an isoelectric point (p*I*) greater than 8, but this phenomenon is common with proteins focusing in the basic range. The masses of proteins detected in microsomes ranged from 10 to 150 kDa, although 8–16% polyacrylamide gels can resolve proteins up to 200 kDa (unpublished observations). Image analysis software showed a comparable total number of stained microsomal proteins for each sample between control and treated males, 239 ± 16 and 267 ± 16 respectively, and between control and treated females, 174 ± 13 and 181 ± 14, respectively. A slightly greater staining intensity of low-expression proteins accounted for the greater number of total microsomal proteins found in males over females.

Proteins were selected for identification by MS on the basis of a 1.5-fold or greater difference from the control in either sex. Of these 48 differentially expressed pro-

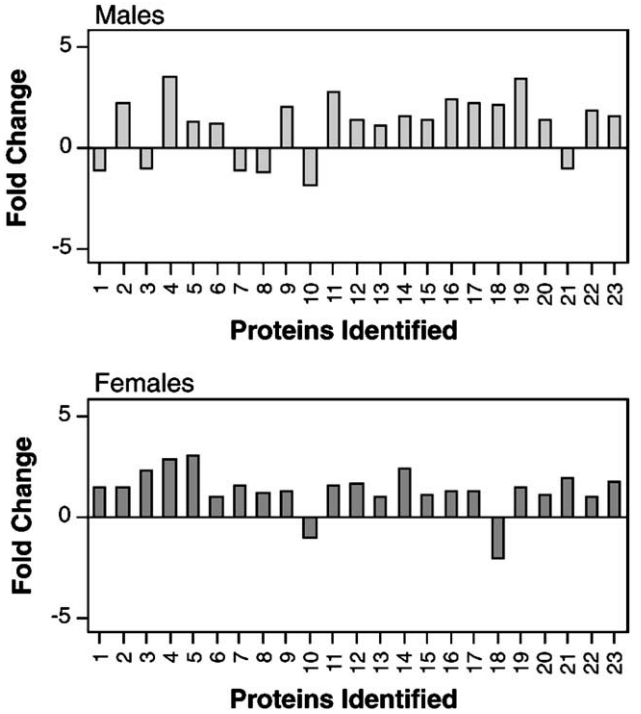

Fig. 3. Differential expression of liver microsomal proteins from stained 2D gels following acute TCDD treatment in male and female Sprague–Dawley rats. Image analysis using PDQuest software identified those proteins that underwent a $\geqslant 1.5$-fold change in expression with TCDD treatment in one or both sexes. Some proteins (6, 8, 13, and 20) were identified by MS analysis for use as landmark proteins and were not differentially expressed in stained gels.

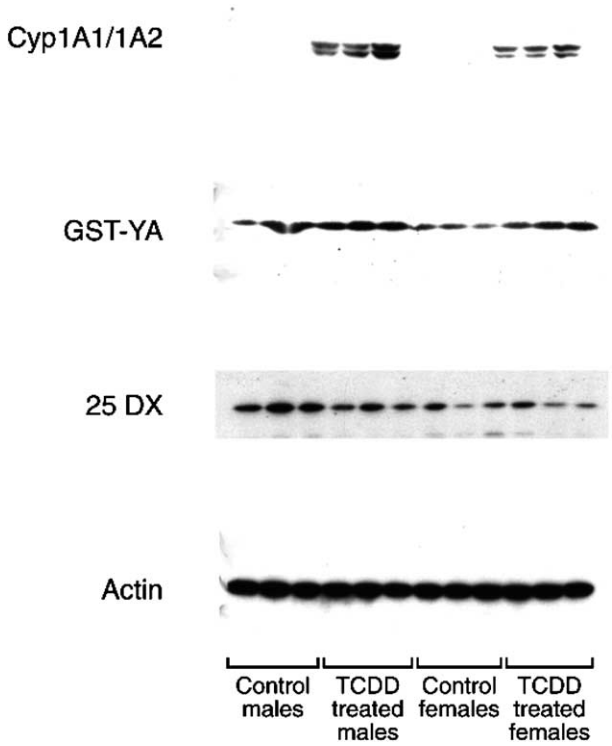

Fig. 4. Effect of TCDD on resident microsomal proteins as measured by western blot. Equal amounts of protein lysate were loaded per lane for each western blot. Each lane represents lysate from an individual animal at 3 rats per group. Both CYP1A1/1A2 and GST-Ya subunit were induced by TCDD treatment. Blots were probed for actin which served as a loading control to show comparability among sample lanes.

teins, we were able to identify by MS nearly one-half (19 proteins) that were reproducibly resolved and detected. The remaining differentially expressed proteins could not be identified due to the lack of major ions in the mass spectrum and low protein levels in the stained gel for analysis. In addition, four proteins were selected as landmarks (proteins 6, 8, 15, and 20 in Table 1) for a total of 23 identified proteins.

Table 1 shows the proteins identified by MS after excision from 2D gels and tryptic digestion. The ratios of the mean staining intensity values (TCDD/control ratio) for each protein in Fig. 3 show the relative difference from control. Proteins from CBB-stained gels that consistently increased in both sexes were heat shock protein (Hsp)72, albumin, glutamate dehydrogenase, isocitrate dehydrogenase, CYP2D4, glyceraldehyde-3-phosphate dehydrogenase, prohibitin, IKK2, PRxIV, GST-Yb2 subunit, and Cu/Zn superoxide dismutase (SOD), while Grp78 and ferritin light chain increased in females only and cytochrome b5 increased in males only.

Western blotting of proteins responding to TCDD

Western blots of microsomal proteins were performed to determine the effect of TCDD treatment upon selected proteins after SDS–PAGE separation. Induction of CYP1A1 and CYP1A2 proteins was clearly observed in each TCDD treated rat compared to undetectable levels observed in control animals (Fig. 4). The basal level of CYP1A expression was below the

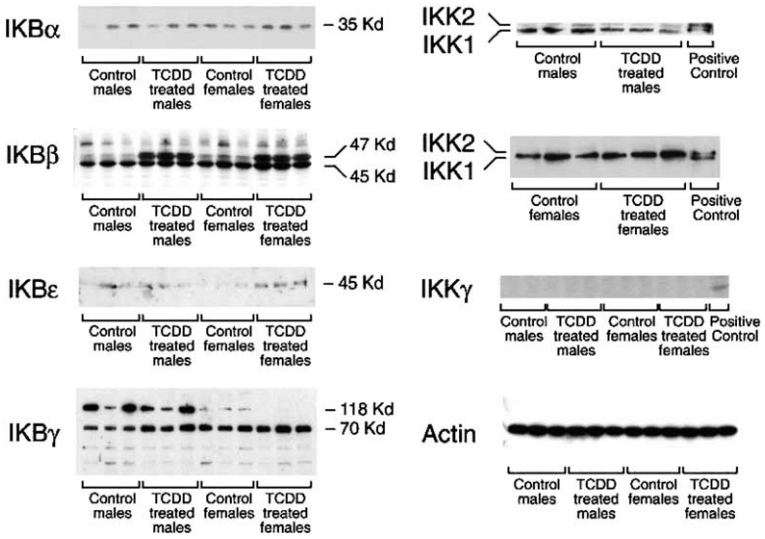

Fig. 5. Effects of TCDD treatment on IκB proteins and IKK subunits found in liver microsomes by western blot. Left panel set: A treatment-related increase in a more slowly migrating form of IκB-β occurred in both male and female rats. Also, a 105-kDa band immunoreactive for IκB-γ was primarily detected in male microsomal samples but was not affected by TCDD treatment. Only low levels of IκBα and no IκBε were found in microsomes. Right panel set: IKK1 was clearly observed in liver microsomes but levels did not change with sex or treatment. IKK2 was expressed in males and was detectable in female samples without discernable treatment effect. IKKγ/NEMO was not detected. HeLa and Jurkat cell lysates served as positive controls for IKK1,2 and IKKγ/NEMO, respectively. Each lane contained lysate from a single animal at three rats per group.

limits of detection in control animals under these conditions. Other responsive proteins measured by densitometry from western blots (Figs. 1 and 4) were the GST-Ya subunit, which increased 5.7- and 2.9-fold, Grp78, which was increased 1.5- and 2.1-fold, and GM130, which was increased by 1.6- and 1.8-fold in females and males, respectively. 25-DX protein showed a slight decrease of $\leqslant$1.3-fold in both sexes.

Effect of TCDD on IκB and IKK expression in microsomes

The finding of IKK2 in microsomes by MS was unexpected because components of the NF-κB pathway such as IκB binding proteins and their associated kinases, are generally assumed to reside in the cytosol and not membranous sites in the cell. We considered the possibility that other members of the IκB and IKK family might be present in the microsomes, and that their expression might be affected by TCDD treatment. Fig. 5 shows the effect of sex and TCDD treatment upon IκB protein expression. IκBβ and IκBγ were the most highly expressed IκB members in microsomes from male and female rats, compared to the low expression levels of IκBα and IκBε. It was notable that TCDD treatment produced a slower migrating band at 47 kDa in all animals of both sexes, consistent with phosphorylated forms of IκBβ found by others [30]. IκBγ, although comparably expressed in both sexes, was unaffected by TCDD exposure. A 105-kDa band reactive with IκBγ antibody, however, was clearly observed in male rats, while it was barely detectable in female controls and absent from female treated rats.

The presence of IKKs in microsomes was also evaluated (Fig. 5) by western blotting. IKK1 was the predominant form expressed in both male and female rats in microsomes. By comparison, IKK2 expression was sevenfold lower than IKK1 in male rats by densitometry of western blots. Although IKK2 could be detected in female microsomes, its expression was at detection limits and was difficult to quantitate. TCDD treatment did not appear to greatly affect the levels of immunostained IKK1 or IKK2. By contrast, IKK2 could be observed in stained 2D gels and was imaged at greater intensity with TCDD treatment. This latter observation may relate to staining properties of the IKK2 protein and its subsequent image analysis over a wide area (streaking) in the basic region of 2D gels (Fig. 2). The noncatalytic subunit, IKKγ/NEMO, could not be detected by western blot from microsomes.

Effect of TCDD on IκB and IKK expression in cytosol

The effects of TCDD and the unique expression pattern of IκB and IKK members in microsomes suggested that we compare the expression pattern of these proteins in cytosol. While little IκBγ was found in cytosol, levels of IκBα, IκBβ, and IκBε were readily detectable (Fig. 6). No differences were found for IκBα and IκBε expression by sex or TCDD treatment; however, more slowly migrating forms of IκBβ were more notable in females than in males, but were not altered by TCDD

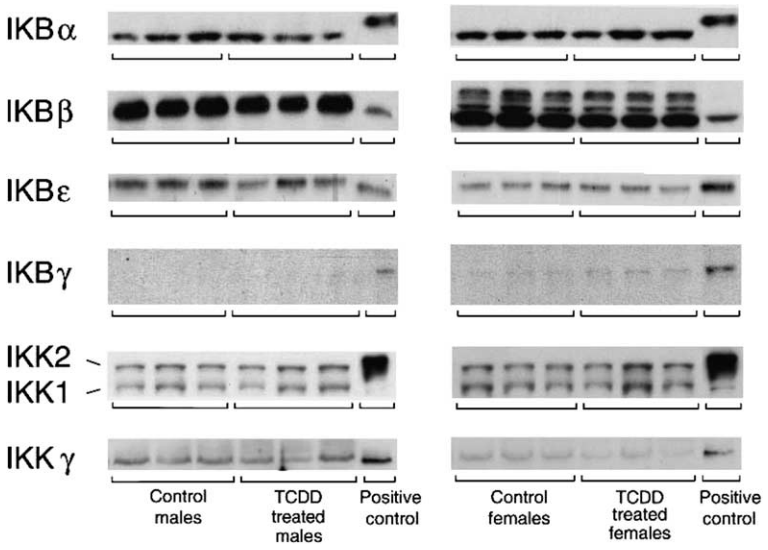

Fig. 6. Effects of TCDD treatment on IκB proteins and IKK subunits found in liver cytosol by western blot. IκBα, IκBβ, and IκBε were found in all cytosolic samples but were not altered by TCDD. Slower migrating forms of IκBβ were observed in female samples only. IκBγ was below the limits of detection. The presence of IKK1, IKK2, and IKKγ/NEMO was observed in cytosol from male and female livers but their levels relative to control did not change with sex or treatment. HeLa and Jurkat cell lysates served as positive controls for IKK1,2 and IKKγ/NEMO, respectively. Each lane contained lysate from a single animal at three rats per group.

treatment. Fig. 6 shows comparable expression among cytosolic IKK1 and IKK2 in both sexes, while cytosolic IKKγ/NEMO expression was relatively lower in females. TCDD treatment did not greatly affect cytosolic IKK protein levels in male or female rats. In general, the relative effects of TCDD treatment and sex upon IκB and IKK protein expression were greater in microsomes than in cytosol.

IKK activity in microsomes and cytosol as affected by TCDD

It was of interest to know if the IKK subunits that were found in the microsomes were catalytically active. IKK kinase activity was determined after immunoprecipitation of IKK1,2-immune complexes from solubilized microsomes or hepatic cytosol (Fig. 7). A full-length IκBα-GST fusion protein served as substrate in the in vitro kinase reaction and was clearly phosphorylated by IKK1,2 from the microsomes, compared to the negative control. Cytosolic IKK1,2 activity was higher than in microsomes by approximately ninefold in both sexes. IKK activity in microsomes is not due to trace cytosolic IKK, as argued by (a) the homogeneity of the microsomal preparation, (b) unique cytosolic and microsomal distribution of IKK and IκB subunits, and

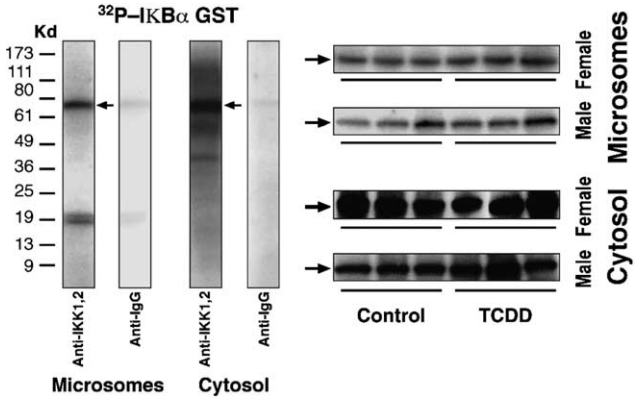

Fig. 7. IκB kinase activity in rat liver cytosol and microsomes. Cytosol and microsomes were freshly isolated from livers of control and TCDD-treated rats as described in Materials and methods. IKK1,2 were immunoprecipitated from 500 μg cytosol or solubilized microsomes. Anti-rabbit IgG antibody was used as a negative control. In vitro kinase activity was performed with ^{32}P-ATP and full-length IκBα-GST protein for 20 min at 30°C. After separation of reaction mixtures by SDS–PAGE, gels were dried and exposed to film. The left panel shows that labeled IκBα-GST (arrows) was the primary ^{32}P product of the kinase reaction. Almost no signal occurred with the nonspecific primary IgG antibody as shown in the adjacent lanes. Data in the left panel are from a representative experiment using cytosol and microsomes from female liver. Samples from male-derived cytosol and microsomes produced similar results (data not shown). The panel sets on the right show ^{32}P-IκBα-GST (arrows) produced from IKK1,2 kinase reactions in microsomes and cytosol lysates from male and female rats. Each lane is a reaction product from an individual animal at three rats per group.

(c) the absence of carry-over of nonspecific kinases in microsomes versus cytosol. Densitometry showed that TCDD treatment increases the IKK kinase activity in males and females, respectively, (21 and 28%) in cytosol and (23 and 12%) in microsomes. These data indicate that a modest increase in IKK kinase activity was produced by TCDD exposure in both sexes.

Discussion

The purpose of this study was to gain new insight into the effects of TCDD toxicity by conducting a proteomic analysis of microsomes. About 220 proteins were stained from microsomes after 2D gel separation with approximately 10% of the detected proteins being expressed at a 1.5-fold difference from control and identified by MS. Proteins that were consistently increased in both sexes were Hsp72, glutamate dehydrogenase, IKK2, isocitrate dehydrogenase, CYP2D4, albumin, glyceraldehyde-3-phosphate dehydrogenase, prohibitin, peroxiredoxin IV, GST Yb2 subunit, and Cu/Zn SOD. Increased levels of these hepatic proteins may reflect increased oxidative stress mediated by TCDD exposure [2–4,31], though the level of knowledge of global protein profiles of oxidant stressors is still in the formative stage. Changes in protein expression measured after dietary protein depletion reportedly produced a pattern of protein alterations in female mouse liver similar to those in our study when analyzed by 2D gel electrophoresis [32]. Such alterations in expression of Cu/Zn SOD, carbonic anhydrase III, CYP450, and several GST isoforms were interpreted as indicative of a diminished liver defense against oxidant stress [32].

Induction of CYP1A1/1A2 in microsomes in this study, as shown by western blot, ensured that each animal responded to the inductive effects of TCDD. Although CYP2D4 was identified during 2D gel electrophoresis, other cytochrome P450 isoforms such as CYP1 were absent due to poor resolution on global 2D gel maps and from their hydrophobic and basic nature [33]. Interestingly, CYP2D4, one of five CYP2D isoforms expressed in rat liver, possesses progesterone hydroxylation activity [34]. Incubation of TCDD with cultured human luteinizing granulosa cells over several days reduced estrogen synthesis, while progesterone and 17-α-hydroxyprogesterone production were unaffected [35]. The steroidogenic effects of increased CYP2D4 in our study are not yet known, although many steroid receptor proteins are present in liver including the membrane-bound progesterone receptor 25-DX. For the first time, 25-DX protein has been identified by 2D gel-MS from microsomes in male and female rat liver as a relatively abundant, acidic ($pI = 4.4$) 25-kDa protein. Previous work had localized this progesterone-binding receptor to the ER and Golgi of porcine hepatocytes by

ligand binding and immunofluorescence [36] and at the plasma membrane in rat hypothalamus [37]. Although prior work reported that 25-DX transcript expression can be up-regulated by TCDD in male rats [26], western blotting revealed a TCDD-related decrease in 25-DX expression in males. Concentrations of 25-DX may exist at various subcellular locations within the hepatocyte and TCDD may differentially affect the subcellular distribution of 25-DX in a manner that does not correlate with mRNA levels. Further proteomic studies at different subcellular locations may be an effective approach for discovering TCDD responsive genes.

A finding of particular interest during proteomic analysis was the presence of IKK2 in microsomes. In most cells, receptor-mediated activation of the IKK complex results in phosphorylation of IκB subunits bound to NF-κB/Rel proteins in the cytoplasm, bringing about degradation of IκBs and nuclear translocation of NF-κB [14,38]. These processes primarily occur within the cytosol and are not generally associated with a specific organelle. A recent study using the yeast two-hybrid system validated an interaction between IκBα and the mitochondrial ATP/ADP translocator ANT [39], a critical component of the mitochondrial permeability transition pore. Further, IκBα was found associated with p65/NF-κB in the mitochondrial intermembrane space [39]. However, no previous studies have reported the presence of NF-κB, IκB, or IKK family members in the microsomes. Here, we have found that microsomes have been enriched for resident proteins of the endoplasmic reticulum and Golgi, while markers for cytosol, mitochondria, nuclei, and plasma membrane were undetectable. Recent research describes an intimate relationship between ER and Golgi such that every component of the Golgi is recycled through the ER, leading some researchers to question if the Golgi apparatus is an ER derivative [40]. While no separation method can lead to complete organelle purity, the present characterization of microsomes and reports of others [36,39,40] were sufficient to lead us to widen our investigation beyond IKK2, to include other members of the NF-κB pathway. The finding that p65-IκBα complexes appear in mitochondria [39] suggests the likelihood of other NF-κB pathway members being present and functioning at cellular sites in addition to cytosol.

This study revealed that expression of IκB binding proteins and IKK was uniquely distributed in hepatic microsomes, in contrast to cytosol, in a TCDD- and sex-specific manner. First, a differential expression of IκB and IKK proteins was observed in cytosolic and microsomal bound subcellular locations. In the microsomes, the predominant NF-κB binding proteins were IκBβ and IκBγ, while in the cytosol IκBα, IκBβ, and IκBε forms were present. In cytosol, IKK subunits were equally represented, while in microsomes, IKK1 and IKK2 were observed but IKKγ was not detected. Second, sex differences were observed in IκBβ and IκB-γ expression. Hyperphosphorylation of IκBβ occurred in females within both microsomes and cytosol. In addition, a high MW band of IκBγ was found in male microsomes that was not found in female rats or in cytosol of either sex. Third, TCDD increased phosphorylation of IκBβ substantially above modest control levels in the microsomes of both males and females. IκBβ phosphorylation was also prominent in female cytosol. Fourth, IKK subunits in microsomes form an active kinase capable of phosphorylating IκB proteins and subject to increased activity by TCDD.

The exact function of IκB and IKK proteins in the microsomes is not yet clear. IκBs are usually bound to NF-κB subunits, although p65 and p50 subunits were not directly observed in the microsomes (Fig. 1 and unpublished data). However, there was evidence for p105 protein in microsomes as a cross-reactive band with anti-IκBγ. The NFκB precursor protein, p105, has a unique role in the control of NF-κB activity because p105 can bind and compete for NFκB inhibitory proteins like IκBs or can be posttranslationally processed to the NFκB subunit, p50 [41]. Alternately, p105 can also be phosphorylated at its C-terminus by IKK for ubiquitin degradation [42,43]. It is possible that p105 in the microsomes might serve as a latent subcellular repository for additional p50 subunits that can be processed and mobilized from p105 in response to specific stimuli.

Another aspect of NF-κB regulation is the phosphorylation of IκBβ, which was affected by TCDD treatment. Many studies have revealed that phosphorylation differentially regulates IκBα and IκBβ binding affinity and degradation. Shortly after extracellular TNFα or interleukin-1 (IL-1) receptor stimulation, IκBα phosphorylation at Ser^{32} and Ser^{36} elicits its rapid degradation, allowing the subsequent nuclear translocation of NF-κB. Alternately, IκBβ interactions are associated with persistent NF-κB effects after release of IκBβ from NF-κB and the resynthesis of a hypophosphorylated IκBβ that sustains NF-κB activation [44–46]. Degradation of IκBβ in murine systems involves phosphorylation by IKK at Ser^{19} and Ser^{23} after stimulation by TNFα or IL-1 receptors or Tax-1 viral protein [47,48] in a similar manner to the -DSXXDS- motif of IκBα [17]. Various reports show up to three separable forms of IκBβ [17] containing hypo- and hyperphosphorylated forms of IκBβ. Although two splice variants are known for human IκBβ, murine IκBβ expression produces only one gene product and the same might be expected for rat. In our study, TCDD produced a slower migrating IκBβ band in the microsomes from both female and male rats, while in cytosol only female rats and not males showed multiple IκBβ forms. These data suggest that IκBβ in females may be under more extensive regulation than in males and could be an

important determinant of female sensitivity to the toxic effects of persistent environmental chemicals like TCDD.

The multimeric IκB kinase complex (IKK) is an important regulator of NF-κB activation by phosphorylating IκBs which leads to their degradation and release from NF-κB. The IKK complex isolated from cytoplasm consists of two catalytic subunits, IKK1 and IKK2, that show about 50% sequence homology and an essential noncatalytic, structural subunit called IKKγ/NEMO. We identified IKK2 from microsomes on the basis of four tryptic fragments from MALDI-MS (three unique peptides and one methoxy peptide) that matched peptides from the predicted sequence for rat IKK2 (NCBI No. 16758078). Western blot analyses of microsomes indicated that the IKK1 subunit was the predominant subunit, with lesser amounts of IKK2, and the IKKγ/NEMO subunit was either absent or below the limits of ECL detection. A potential IκB kinase function of IKK1 and IKK2 in microsomes was suggested by the in vitro kinase assay performed in this study. The finding of kinase activity in microsomes in the absence of IKKγ/NEMO, considered essential for in vivo kinase activity, was unexpected. However, prior work has shown that either recombinant IKK1 or IKK2 separately possess kinase activity in vitro, with IKK2 being the more catalytically active of the two. In IKKγ/NEMO$^{-/-}$ fibroblasts, a small amount of IKK kinase activity is still observed [49,50] and might be explained by the formation of IKK1 and IKK2 dimers in the cytosol and microsomes. It is recognized that the process of solubilizing the microsomal membranes may create IKK1 or IKK2 homodimers with kinase activity that may not exist in vivo. However, the membrane environment of the microsomes may also provide a natural structural integrity to allow IKK1 and IKK2 dimerization and kinase activity under normal cellular conditions. Studies are in progress to evaluate these possibilities. Also under consideration is the intriguing prospect that IKK function in microsomes, especially that of IKK1, may be unrelated to IκB kinase activity. Biochemical and gene deletion studies indicate each IKK may have differing physiological functions. IKK2 and IKKγ/NEMO are required for activating NF-κB by proinflammatory stimuli and preventing apoptosis induced by TNFα. IKK1 is dispensable for these functions but is essential for development and differentiation, in particular keratinocyte differentiation that is independent of IKK1-mediated kinase activity or interaction with IKKγ/NEMO [51]. Instead of acting through IKK or NF-κB activation, IKK1 controls the production of a differentiation-inducing factor for epidermal differentiation [51]. The modest increases in IKK kinase activity from TCDD reported here might also have consequences for complex cellular programs such as differentiation after long-term TCDD exposure.

The possible function of IκB and IKK proteins in the microsomes and their relationship to TCDD toxicity should be explored on a cell-, tissue-, and organ-specific basis. The functional significance of IκB and IKK proteins in microsomes and their relationship to TCDD toxicity will become clearer with further experiments that perturb the NF-κB pathway. Overall, this study shows that proteomic technologies can be effectively used as a discovery-oriented tool to generate new hypotheses. The testing and refinement of such new hypotheses will strengthen the predictive value of animal models in experimental biology and further our understanding of the effects of toxicant exposure upon human health.

Acknowledgments

The authors greatly appreciate the contribution by Dr. Douglas A. Bell at the NIEHS of the 25-DX antibody used in this study. Constructive comments and suggestions in review of the manuscript from Drs. Tish Murphy and Michael L. Cunningham were invaluable in shaping the manuscript. Critical discussions and support of this work by Drs. Paul Nettesheim, Raymond W. Tennant, and James K. Selkirk are gratefully acknowledged.

References

[1] S. Safe, Toxicol. Lett. 120 (2001) 1–7.
[2] C. Delescluse, N. Ledirac, R. Li, M.P. Piechocki, R.N. Hines, X. Gidrol, R. Rahmani, Biochem. Pharmacol. 61 (2001) 399–407.
[3] H.G. Shertzer, D.W. Nebert, A. Puga, M. Ary, D. Sonntag, K. Dixon, L.J. Robinson, E. Cianciolo, T.P. Dalton, Biochem. Biophys. Res. Commun. 253 (1998) 44–48.
[4] M.E. Wyde, S.R. Eldridge, G.W. Lucier, N.J. Walker, Toxicol. Appl. Pharmacol. 173 (2001) 7–17.
[5] National Toxicology Program, Bioassay of 2,3,7,8-Tetrachlorodibenzo-*p*-dioxin for Possible Carcinogenicity (Gavage Study). National Toxicology Program at NIEHS, Research Triangle Park, NC, 1982.
[6] R.J. Kociba, D.G. Keyes, J.E. Beyer, R.M. Carreon, C.E. Wade, D.A. Dittenber, R. Kalnins, L.E. Frauson, C.N. Park, S.D. Barnard, R.A. Hummel, C.G. Humiston, Toxicol. Appl. Pharmacol. 46 (1978) 279–303.
[7] B.I. Yoon, Y. Hirabayashi, T. Kaneko, Y. Kodama, J. Kanno, J. Yodoi, D.Y. Kim, T. Inoue, Arch. Environ. Contamin. Toxicol. 41 (2001) 232–236.
[8] B.J. Connell, A. Singh, I. Chu, J. Submicrosc. Cytol. Pathol. 30 (1998) 157–163.
[9] A. Bowie, L.A. O'Neill, Biochem. Pharmacol. 59 (2000) 13–23.
[10] P.A. Baeuerle, T. Henkel, Annu. Rev. Immunol. 12 (1994) 141–179.
[11] P.A. Baeuerle, D. Baltimore, Cell 87 (1996) 13–20.
[12] L.A. O'Neill, C. Kaltschmidt, Trends Neurosci. 20 (1997) 252–258.
[13] W.C. Sha, J. Exp. Med. 187 (1998) 143–146.
[14] M.W. Mayo, A.S. Baldwin, Biochim. Biophys. Acta 1470 (2000) M55–M62.

[15] S. Yamazaki, T. Muta, K. Takeshige, J. Biol. Chem. 276 (2001) 27657–27662.
[16] H.L. Pahl, Oncogene 18 (1999) 6853–6866.
[17] R. Weil, C. Laurent-Winter, A. Israel, J. Biol. Chem. 272 (1997) 9942–9949.
[18] C.E. Sulentic, M.P. Holsapple, N.E. Kaminski, J. Pharmacol. Exp. Ther. 295 (2000) 705–716.
[19] Y. Tian, S. Ke, M.S. Denison, A.B. Rabson, M.A. Gallo, J. Biol. Chem. 274 (1999) 510–515.
[20] A. Puga, S.J. Barnes, T.P. Dalton, C. Chang, E.S. Knudsen, M.A. Maier, J. Biol. Chem. 275 (2000) 2943–2950.
[21] A. Puga, A. Maier, M. Medvedovic, Biochem. Pharmacol. 60 (2000) 1129–1142.
[22] J.E. Celis, M. Kruhoffer, I. Gromova, C. Frederiksen, M. Ostergaard, T. Thykjaer, P. Gromov, J. Yu, H. Palsdottir, N. Magnusson, T.F. Orntoft, FEBS Lett. 480 (2000) 2–16.
[23] A. Pandey, M. Mann, Nature 405 (2000) 837–846.
[24] F.S. Heinemann, J. Ozols, Front. Biosci. 3 (1998) D483–D493.
[25] N.J. Walker, F.G. Crofts, Y. Li, S.F. Lax, C.L. Hayes, P.T. Strickland, G.W. Lucier, T.R. Sutter, Carcinogenesis 19 (1998) 395–402.
[26] O. Selmin, G.W. Lucier, G.C. Clark, A.M. Tritscher, J.P. Vanden Heuvel, J.A. Gastel, N.J. Walker, T.R. Sutter, D.A. Bell, Carcinogenesis 17 (1996) 2609–2615.
[27] B.A. Merrick, W. Zhou, K.J. Martin, S. Jeyarajah, C.E. Parker, J.K. Selkirk, K.B. Tomer, C.H. Borchers, Biochemistry 40 (2001) 4053–4066.
[28] R.F. Schwabe, B. Schnabl, Y.O. Kweon, D.A. Brenner, J. Immunol. 166 (2001) 6812–6819.
[29] N. Nakamura, M. Lowe, T.P. Levine, C. Rabouille, G. Warren, Cell 89 (1997) 445–455.
[30] A. Venkatakrishnan, A.A. Stecenko, G. King, T.R. Blackwell, K.L. Brigham, J.W. Christman, T.S. Blackwell, Am. J. Resp. Cell Mol. Biol. 23 (2000) 396–403.
[31] S. Cho, Y. Kim, M.O. Cruz, E.M. Park, C.K. Chu, G.Y. Song, T.H. Joh, GLIA 33 (2001) 324–333.
[32] P.M. Sanllorenti, J. Rosenfeld, V.P. Ronchi, P. Ferrara, R.D. Conde, Mol. Cell. Biochem. 220 (2001) 49–56.
[33] A.T. Drahushuk, B.P. McGarrigle, K.E. Larsen, J.J. Stegeman, J.R. Olson, Carcinogenesis 19 (1998) 1361–1368.
[34] T. Hiroi, W. Kishimoto, T. Chow, S. Imaoka, T. Igarashi, Y. Funae, Endocrinology 142 (2001) 3901–3908.
[35] F.M. Moran, A.J. Conley, C.J. Corbin, E. Enan, C. VandeVoort, J.W. Overstreet, B.L. Lasley, Biol. Reprod. 62 (2000) 1102–1108.
[36] E. Falkenstein, K. Schmieding, A. Lange, C. Meyer, D. Gerdes, U. Welsch, M. Wehling, Cell. Mol. Biol. (Noisy-le-grand) 44 (1998) 571–578.
[37] C.J. Krebs, E.D. Jarvis, J. Chan, J.P. Lydon, S. Ogawa, D.W. Pfaff, Proc. Natl. Acad. Sci. USA 97 (2000) 12816–12821.
[38] F. Chen, V. Castranova, X. Shi, Am. J. Pathol. 159 (2001) 387–397.
[39] V. Bottero, F. Rossi, M. Samson, M. Mari, P. Hofman, J.F. Peyron, J. Biol. Chem. 276 (2001) 21317–21324.
[40] S. Miles, H. McManus, K.E. Forsten, B. Storrie, J. Cell. Biol. 155 (2001) 543–555.
[41] C.M. Fan, T. Maniatis, Nature 354 (1991) 395–398.
[42] V. Heissmeyer, D. Krappmann, F.G. Wulczyn, C. Scheidereit, EMBO J. 18 (1999) 4766–4778.
[43] A. Orian, H. Gonen, B. Bercovich, I. Fajerman, E. Eytan, A. Israel, F. Mercurio, K. Iwai, A.L. Schwartz, A. Ciechanover, EMBO J. 19 (2000) 2580–2591.
[44] R.J. Phillips, S. Ghosh, Mol. Cell. Biol. 17 (1997) 4390–4396.
[45] H. Suyang, R. Phillips, I. Douglas, S. Ghosh, Mol. Cell. Biol. 16 (1996) 5444–5449.
[46] J.E. Thompson, R.J. Phillips, H. Erdjument-Bromage, P. Tempst, S. Ghosh, Cell 80 (1995) 573–582.
[47] J. DiDonato, F. Mercurio, C. Rosette, J. Wu-Li, H. Suyang, S. Ghosh, M. Karin, Mol. Cell. Biol. 16 (1996) 1295–1304.
[48] T.A. McKinsey, J.A. Brockman, D.C. Scherer, S.W. Al-Murrani, P.L. Green, D.W. Ballard, Mol. Cell. Biol. 16 (1996) 2083–2090.
[49] D. Rudolph, W.C. Yeh, A. Wakeham, B. Rudolph, D. Nallainathan, J. Potter, A.J. Elia, T.W. Mak, Genes Dev. 14 (2000) 854–862.
[50] Y. Hu, V. Baud, M. Delhase, P. Zhang, T. Deerinck, M. Ellisman, R. Johnson, M. Karin, Science 284 (1999) 316–320.
[51] Y. Hu, V. Baud, T. Oga, K.I. Kim, K. Yoshida, M. Karin, Nature 410 (2001) 710–714.